Dynamic Analysis of V Transmission Lines

Omar M. Ramahi, Atef Z. Elsherbeni, *Senior Member, IEEE,*
and Charles E. Smith, *Life Senior Member, IEEE*

***Abstract*— In this work, a dynamic analysis of the V line is presented. Previous work analyzed the performance of this structure for low frequency applications using quasistatic approximations. Here, we extend the analysis of the V line into the higher frequency range where dispersion becomes significant and where it cannot be predicted by quasistatic methods. We show that the V line provides features and advantages that are not present in the conventional microstrip structures, most notably the appreciable decrease in coupling between adjacent lines in comparison with the conventional microstrip structure. This feature makes the V line well suited for high packaging density applications. The full-wave analysis is carried out using a Yee-cell based finite-difference time-domain (FDTD) method, while enforcing a highly efficient and stable mesh truncation technique. Results are presented for a single and multiconductor structures.**

***Index Terms*— Dispersion, finite-difference time-domain, numerical modeling, packaging, transmission lines.**

I. Introduction

THE increase in packaging density and clock speed reaching into the GHz region created a need for transmission media that occupies less space while maintaining the desired performance. Several unconventional structures were proposed in the literature [1]–[5], amongst which is the V line shown in Fig. 1. The major geometrical features of the V line are the angle α that defines the isosceles triangle of the V-shaped groove, the width W of the signal line (trace), and the composition and thickness H of the dielectric substrate. For instance by varying the angle α, the characteristic impedance of the line and the effective permittivity can be affected while maintaining a fixed substrate material and thickness. Also, the closer proximity of the ground plane to the signal conductor is an attractive feature from the signal integrity standpoint, since this leads to a reduction in the electromagnetic coupling and consequently minimization of crosstalk between adjacent lines [1].

These new transmission line configurations, and especially the V line, have thus far been analyzed through conformal mapping techniques and integral equations methods while assuming quasi-TEM field behavior [1], [5]. However under the quasistatic assumption, the dispersive nature of these structures and other important propagation features (full-wave effects) cannot be accounted for. For structures that operates into the GHz region, dispersive behavior and Ohmic losses can significantly vary over the bandwidth of interest.

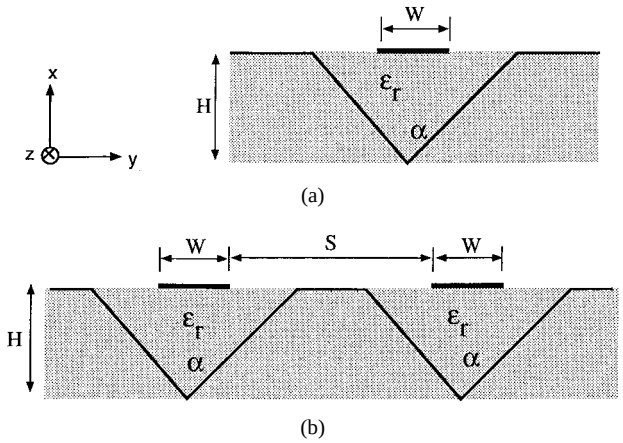

Fig. 1. Cross section of the V line: (a) single V line and (b) multiconductor V line structure.

In this work, we extend the analysis of the V line structure to the GHz regime. The analysis is facilitated by the use of a Yee-cell based finite-difference time-domain (FDTD) method in the Cartesian coordinates system. The strengths of the FDTD method are: first, it can comfortably model intricate irregular geometries such as inclined reference planes. Second, it gives the performance of the structure over a very wide band of frequencies in a single computer simulation. Furthermore, for the purpose of characterization of the structure under study and other similar transmission media, the FDTD method can be made memory-efficient by the application of effective absorbing boundary condition (ABC) that can be made stable [6].

It is emphasized that the three-dimensional (3-D) FDTD method based on the Yee cell was chosen for the study in this work. Alternatively, the 2D-FDTD method can be used to treat transmission lines with uniform cross sections [7], or even the finite element time-domain method. Our choice of the 3-D FDTD method is primarily due to its simplicity and strength and for the fact that it allows for easy extension to treat transmission line discontinuities. Therefore, the usefulness of the 3-D FDTD method as part of a CAD tool extends beyond the primary focus of our work in this paper.

II. Formulation

The FDTD method has been successfully applied to the analysis of microstrip transmission line structures and has proven to be a reliable and robust technique for these problems. (There are many excellent papers on the use of FDTD in transmission line structures; see [8]–[10] for example.) Therefore, the details of the FDTD method are henceforth bypassed. For the application in this work, however, we focus on

Manuscript received October 20, 1997; revised March 28, 1998. This work was supported by Digital Equipment Corporation and the Army Research Office under Grant DAAH04-94-G-0355.

O. M. Ramahi is with Digital Equipment Corporation, Maynard, MA 01754 USA (email: Omar.Ramahi@digital.com).

A. Z. Elsherbeni and C. E. Smith are with the Electrical Engineering Department, University of Mississippi, University, MS 38677 USA (email: atef@sphinx.ee.olemiss.edu).

Publisher Item Identifier S 1070-9894(98)04783-5.

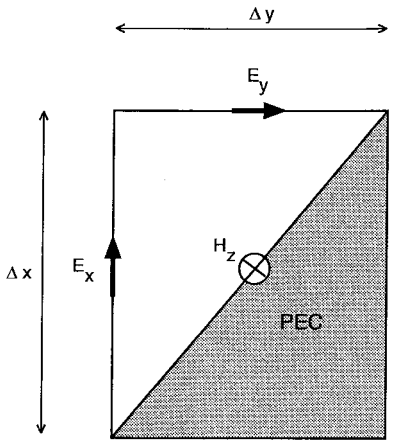

Fig. 2. Cross section of the Yee cell in the x–y plane showing the PEC interface.

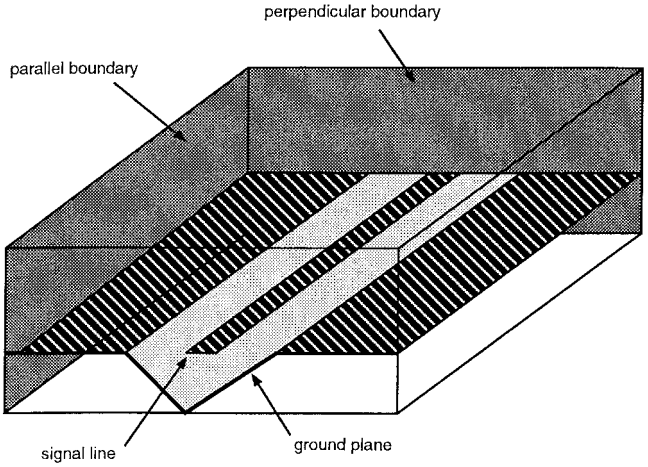

Fig. 3. FDTD computational domain.

the electromagnetic modeling aspects. More specifically, the modeling of the inclined reference plane, the mesh truncation scheme necessary to obtain a finite geometry for FDTD simulation, and the source of energy needed to excite the line.

A. Inclined Surfaces

The nonrectangular, or inclined sections of the ground plane present in the V line are modeled using two different techniques. In the first, the angled surface is approximated using the stair-case technique. In the second, the polygonal approximation is employed [11]. The polygonal approximation is very simple to implement and is highly versatile; however, its drawback (and those of other curved-boundary techniques) is that for resonant structures requiring very large number of time steps, their is a potential for instability [11]–[14]. (A recent work by Craddock and Railton [15] gives an improved angled-surface formulation that promises to eliminate the instability problem.) However, as evident from this work, instability due to the polygonal approximation was not present when analyzing the V line structure.

The implementation of the polygonal approximation is very simple when the cross section of the structure is uniform. Assuming propagation in the z-direction, and thus a cross section in the x–y plane, then following [11], and assuming the perfect electric conductor (pec) ground plane to intersect the cross section of an FDTD Yee cell as shown in Fig. 2, the H_z component is updated in the FDTD scheme according to the formula

$$H_z^{n+1/2}(i+1/2, j+1/2, k) = H_z^{n-1/2}(i+1/2, j+1/2, k) + \frac{2\Delta t}{\Delta x \Delta y} \cdot \left[E_x^n(i+1/2, j+1, k)\Delta x + E_y^n(i, j+1/2, k)\Delta y\right]. \quad (1)$$

This simple formulation does not involve any more calculation than would be required using the standard FDTD staircase approximation, and it can be directly incorporated into an FDTD code. A modeling limitation posed by the polygonal approximation is that the cell size needs to be carefully considered in advance to allow for proper fitting of the inclined metallic boundary such that it coincides with the H_z component. Nevertheless, this is a minor drawback compared to the implementation effort, cost and limitations of other techniques [12]–[15].

B. Mesh Truncation

The next step is to employ a mesh truncation technique in order to limit the extent of the infinite domain of the problem to a finite size. For the problem at hand, the objective is to characterize the propagating and dispersive behavior of the transmission line. The characteristics of the line such as its effective permittivity and characteristic impedance are wholly dependent on the cross section of the line and the substrate permittivity, and are totally independent of the terminations that are typically part of the complete electronic circuitry in which the line is embedded. To determine these characteristics, the effects, physical or artificial, of any terminations to the line have to be absent from the numerical results. The most efficient way to accomplish this is to impose boundary conditions that intersect the propagation direction, thus simulating a line extending to infinity. Of course, the remaining three surfaces (the fourth is a ground plane) have to be treated with boundary conditions, however, their termination plays a less important role. For easy reference, we shall refer to the two boundary surfaces that are perpendicular to the line as the *perpendicular* boundaries, whereas the remaining boundary surfaces as the *parallel* boundaries. The FDTD computational domain is shown in Fig. 3.

While the implementation of a good mesh truncation technique is highly important in all open-region FDTD simulations, the characterization of a transmission line using FDTD imposes further constraints. This is because the transmission line is extended into the perpendicular boundary causing the fields that interact with this boundary to behave in a unique and semi-deterministic fashion. More specifically, the boundary condition imposed on the perpendicular boundary has to achieve three objectives:

1) it has to absorb waves traveling at different speeds which is typical in dispersive microstrip transmission media;
2) it has to be memory-efficient, meaning that it can be applied at terminal boundaries that allow the geometry

to be small-enough to capture the physical behavior of fields;

3) the method should not lead to numerical instability. The third criterion is generally an important one when using FDTD simulation, however, it manifests itself prominently when studying transmission media since a large run time is crucial for capturing the frequency domain behavior over a wide band.

Earlier work found that Higdon's ABC can be effective for analyzing microstrip line structures [16]–[18]. However, in these previous implementations, the effectiveness of the ABC was found to be highly dependent on good prediction of the effective permittivity of the medium over the frequency band of interest. This unfortunately puts a severe limitation on the general applicability of those previous formulations. Furthermore, higher order ABC's, especially of the Higdon type, give higher accuracy, unfortunately their previous applications gave highly unstable simulations.

More recently, the perfectly matched layer (PML) method and the complementary operators method (COM) were applied to terminate the computational domain in all directions [19], [20]. Both of these techniques are effective, however at the expense of increasing the cost of the simulation in terms of computer memory requirements and run time. For the class of electromagnetics problems in this work, i.e., the characterization of printed circuit transmission lines, it is discovered that an elaborate mesh termination technique such as the COM and PML is unnecessary.

A boundary condition formulation that addresses the stringent criteria stated above has recently been presented [6]. This new formulation takes advantage of the field behavior in the guiding structure by employing a fourth-order Higdon ABC on the perpendicular boundaries [16]. This ABC is given by

$$\prod_{i=1}^{N}[\partial_x + (a_i/c)\partial_t]U = 0 \tag{2}$$

where $N = 4$, c is the speed of light, a_i is a constant that can be chosen to reflect the range of propagation velocities that are induced by the structure, and U is the electric field component which is tangential to the boundary. It is important to emphasize that unlike previous work ([17] and [18]), the constant a_i was set to 1 and not optimized based on any *a priori* behavior of the field. This is because here we are using a fourth-order Higdon ABC which gives very small artificial reflections, whereas in previous work, only a second-order ABC was used [17], [18]. Higdon ABC's such as third- and fourth-order ABC's were avoided in the past because they were believed and found to lead to instabilities that became worse as the order of the boundary condition was increased. It is because of such instability that an additional damping factor was added to these boundary condition giving the new form

$$\prod_{i=1}^{N}[\partial_x + (a_i/c)\partial_t + \alpha_i]U = 0. \tag{3}$$

What is crucial to point out here is that for fields that are predominantly propagating, the introduction of the α_i can be a nuisance since it is directly detrimental to lower frequency fields. Despite this, however, the introduction of the α_i's was thought to be a necessary step to maintain stability. It will be shown next that the introduction of the α_i is only necessary to accelerate the absorption of fields incident on the parallel boundaries, which consequently ensures stability.

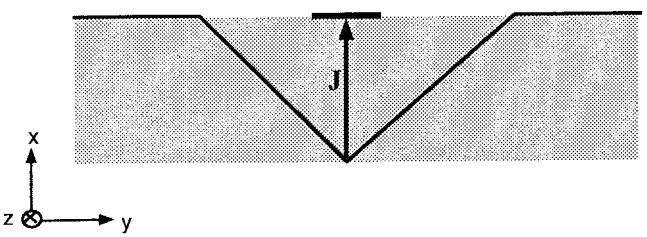

Fig. 4. Impressed current source, **J** between the reference plane and the signal trace.

Shifting focus to the parallel boundaries, it is noted that those surfaces do not intersect any part of the structure and can thus be expected to be less restrictive than the perpendicular boundaries. In fact, the parallel surfaces can be positioned at a distance from the line such that any consequent artificial reflection (mostly evanescent waves) is minute. (In contrast, the perpendicular surfaces intersect the propagating field no matter how far they are positioned.)

Since the waves that are incident on the parallel boundaries are of evanescent nature, the addition of α_i in the boundary condition becomes essential to reduce the evanescent waves. The values of α_i were found empirically to depend on the cell size and can range from $\alpha_i = 0.02/\Delta$ to $\alpha_i = 0.1/\Delta$ where Δ is the cell size in the direction normal to the boundary. It was found that with this choice of α_i, a fourth-order ABC of the type shown in (3) can be enforced at the parallel boundaries while maintaining high accuracy and stability.

Overall, the unique, yet very general and robust, combination of ABC's enforced on the perpendicular and parallel boundaries lead to highly reliable results as demonstrated in the section on numerical results. In fact, stability was observed even when the simulation was run for more than 3000 time steps which was more than sufficient to capture the behavior of the dominant mode.

C. Excitation

The V line is excited by an x-directed impressed current source positioned normal to the trace as shown in Fig. 4 such that it spans the cells extending from the reference plane to the signal line. The primary objective of using a current source—or any source for that matter—in the present simulation is to induce the dominant mode. Therefore, the current source is positioned precisely in the center of the line, as shown in Fig. 4, in order not to stir any undesired higher order modes.

The current line source is positioned ten cells from the near end of the line such that any reflections that are generated from this end due to the ABC can be considered as an integral part of the incident wave form. Since the impressed current source is invisible to fields, that is it has no scattering features, any returning waves (encountered in the study of

line discontinuities or junctions) will pass through without any spurious reflections.

D. Characteristic Impedance, Effective Permittivity, and Coupling Coefficient

The characteristic impedance and effective permittivity were calculated using the Fourier transforms of the appropriate samples of the field along the line in the manner fully described in [8]. The Characteristic Impedance is the ratio of the Fourier transformed voltage to the Fourier transformed current. The voltage and the current time waveforms are calculated at approximately 70 space cells from the source location in order to minimize the effects of higher order modes which typically dominate in the close proximity of the source.

The effective permittivity is calculated from the field samples at two different points along the line such that both points lie where the dominant mode is present.

The coupling between two adjacent lines can be measured using different schemes. Since the interest here is the coupling between two lines that are assumed to be infinite in extent, a useful measure is defined as

$$\text{coupling coefficient} = \frac{V_p}{V_a} \tag{4}$$

where V_p and V_a are the voltages in the passive and active lines, respectively. Again, and in a manner consistent with the calculation of the impedance and permittivity, V_p and V_a are calculated close to the far end of the line.

III. Numerical Results

As an example of a V line structure, we consider a line with the following dimensions.

1) Width of signal line, $W = 0.318$ mm.
2) Thickness of the signal line is zero.
3) Height of substrate, $H = 0.610$ mm.
4) Dielectric constant of substrate, ϵ_r =2.55.

For single and multiconductor line structures, the computational domain was chosen such that the upper boundary was 14 cells from the dielectric-air interface, and the side boundaries were 15 cells from the edge of the nearest signal trace. The number of cells in the propagation direction was chosen to allow for good sampling of the dominant mode for accurate impedance and permittivity calculations, which typically would be around 100 cells.

The dimensions of the FDTD cells were chosen as follows: $\Delta x = 0.0545$ mm, $\Delta z = 0.0318$ mm, and Δy is adjusted to give the desired angle α. The time step is set to $\Delta t = 0.06$ ps. The excitation pulse is a standard Gaussian with a width of 20 Δt, sufficient enough for predicting the frequency response up to 300 GHz. The pulse is shifted in time such that its peak occurs at the 50th time step in order to minimize high frequency errors.

A. Single Line Structure

Initially, the polygonal approximation model for the curved inclined boundaries was validated by making a comparison with the results obtained using the conventional staircase approximation. Fig. 5 shows the characteristic impedance and the effective permittivity for the line having the parameters given above, with $\alpha = 60°$. We observe that the staircase approximation has an effect on the FDTD results only at the higher end of the spectrum. This is an expected outcome since staircase approximations give an increasing error as the wavelength approaches the dimension of the cell.

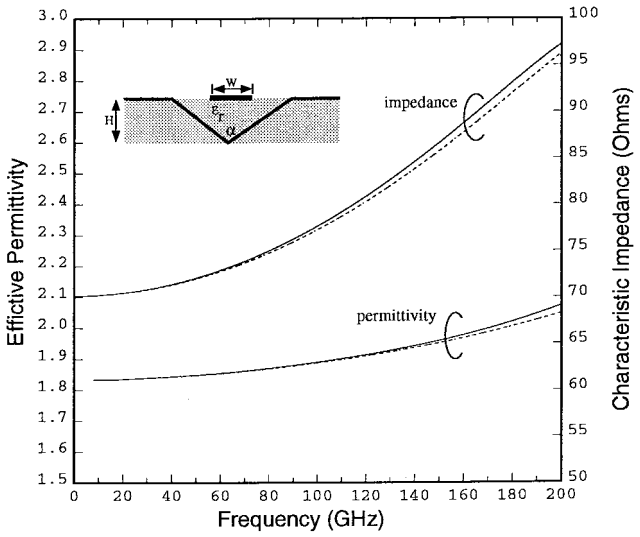

Fig. 5. Calculated values of the characteristic impedance for the V line and the effective permittivity with $\alpha = 60°$ and $W/H = 0.52$. Solid line: staircase approximation. Dashed line: polygonal approximation.

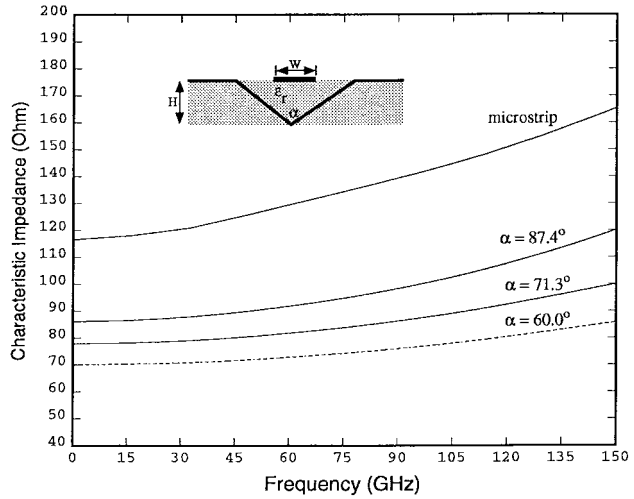

Fig. 6. Calculated values of the characteristic impedance of the V line for different values of α. $W/H = 0.52$.

In Figs. 6 and 7, we show a comparison between a microstrip line and a V line having identical ratios of W/H while varying the angle α. It is clear from these results that the V line becomes less dispersive than the microstrip as the angle α decreases. Notice that as α decreases, the side reference planes approach the signal line, and in essence the structure will have high resemblance to the coplanar line, which is already known to be less dispersive than microstrip lines. As the value of α increases, the V line become more dispersive, however this is of a minor consequence since having a large α creates an

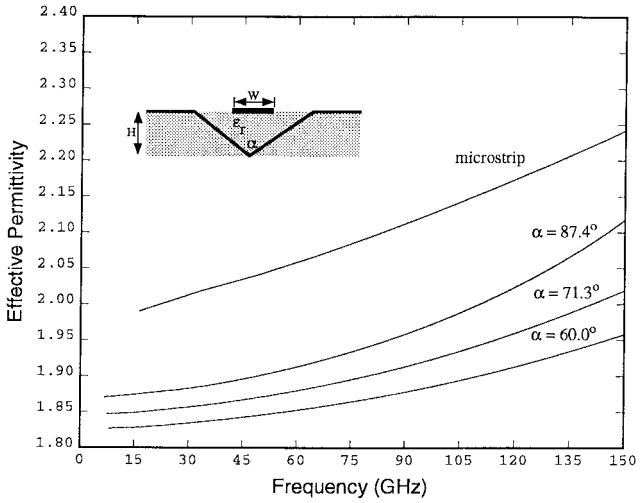

Fig. 7. Calculated values of the effective permittivity of the V line for different values α. $W/H = 0.52$.

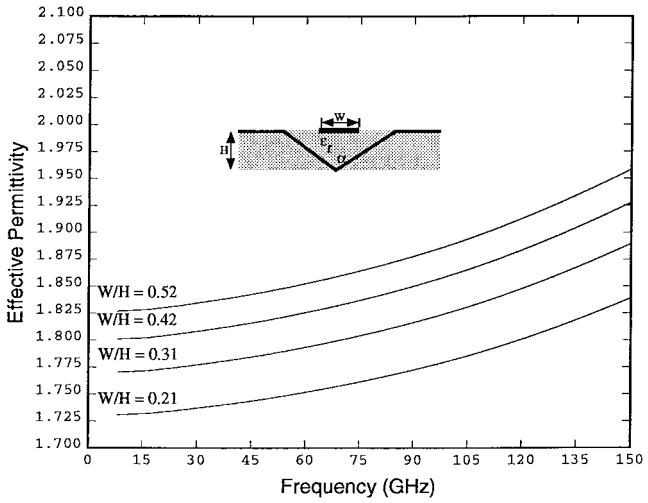

Fig. 9. Calculated values of the effective permittivity of the V line for different ratios W/H. $\alpha = 60°$.

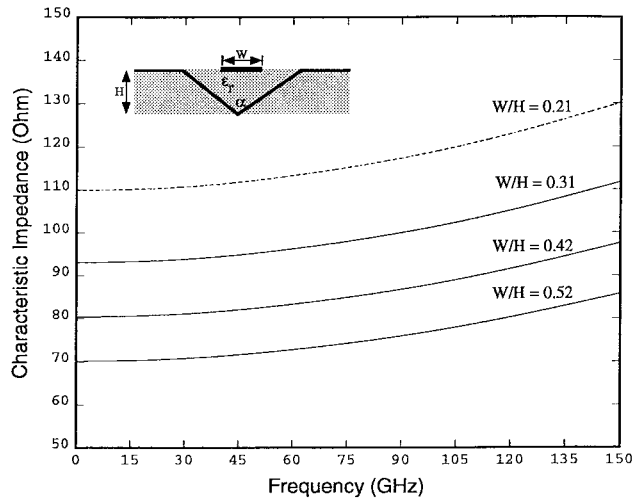

Fig. 8. Calculated values of the characteristic impedance of the V line for different ratios of W/H. $\alpha = 60°$.

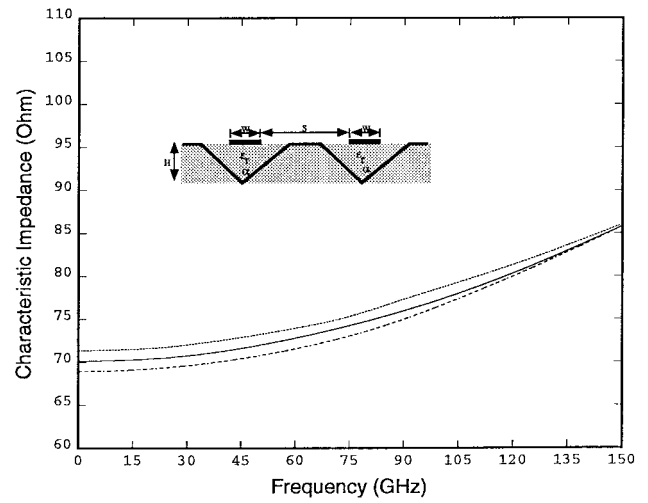

Fig. 10. Calculated values for the characteristic impedance for two identical V lines. $\alpha = 60°$, W/H = 0.52 and $S = 2$ W. Solid line: single mode, dotted line: even mode, and dashed line: odd mode.

impractical structure since it increases the separation between the signal traces in a multiconductor system. This counters our efforts of obtaining higher density packaging in the first place.

There is no measurements available in the literature to compare the behavior of the V line to cover the frequency band of interest of 0–150 GHz. However, for the case of $W/H = 0.52$ and $\alpha = 60°$, the values obtained using FDTD at the lower end of the spectrum are relatively close to those obtained by Schutt–Aine using quasistatic approximations [1]. Our calculation for the impedance at the lower end (dc to 1 GHz) gives 71 Ω for the characteristic impedance, whereas the values measured and calculated by Schutt–Aaine were 76 and 78 Ω, respectively. A similar discrepancy was also observed in the calculation of the effective permittivity. It is noted here that the quasistatic technique used in [1] did not take into account the ground plane extensions (which are on the same plane as the signal conductor). Another source of discrepancy between the measurements in [1] and our numerical calculations can be attributed to the nonexact dielectric constant of the substrate and measurements uncertainties [20]. Despite this, however, we have used a quasistatic analysis tool and found that the characteristic impedance for this test case was 69.8 Ω, which agrees very closely to our FDTD result of 71 Ω.

Figs. 8 and 9 show the effect of varying the ratio W/H on the characteristic impedance and effective permittivity for the V line while keeping the angle α fixed at 60°. Here we notice a similar trend to what was obtained earlier in that as the separation between the edges of the trace and the reference plane decreases, the line becomes less dispersive.

B. Multiconductor Structure

A primary interest in the V line structure is its coupling characteristics when two or more lines are placed in a multiconductor configuration as shown in Fig. 1(b). Here we study the performance of two identical adjacent lines separated by a distance S (see Fig. 1). Fig. 10 gives the characteristic impedance for the even and odd modes. The impedance for the even and odd modes are calculated by having a current line source under each of the two lines in a manner similar to the single line case. For the even mode, the lines are excited

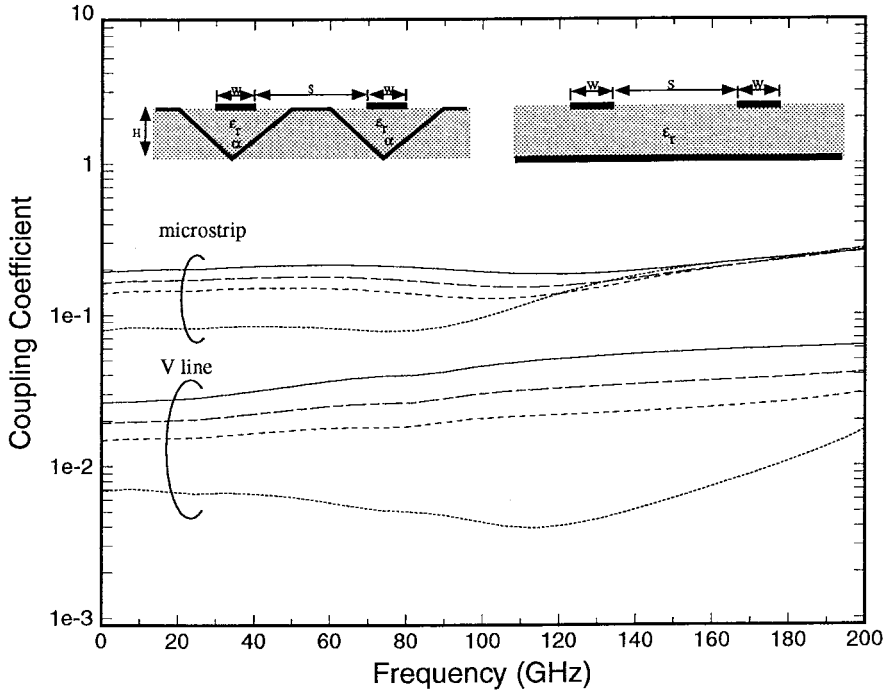

Fig. 11. Coupling coefficient versus frequency for two identical lines for different separation distance S. Solid line: $S = 1.4$ W, long dashes line: $S = 1.7$ W, short dashes line: $S = 2$ W, and dotted line: $S = 3.2$ W.

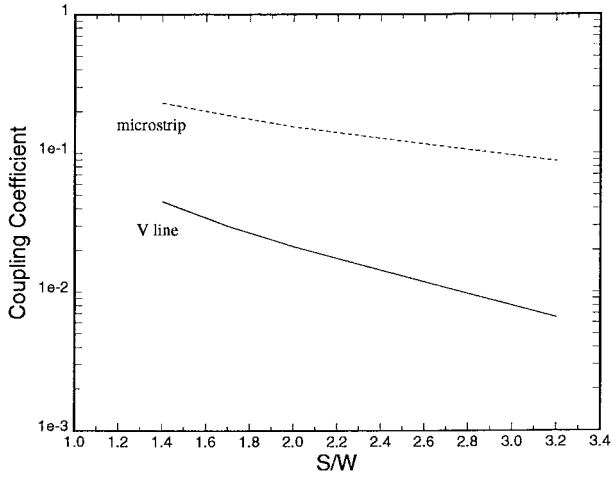

Fig. 12. Coupling coefficient versus spacing between the two lines, S, at 80 GHz. $\alpha = 60°$ and $W/H = 0.52$.

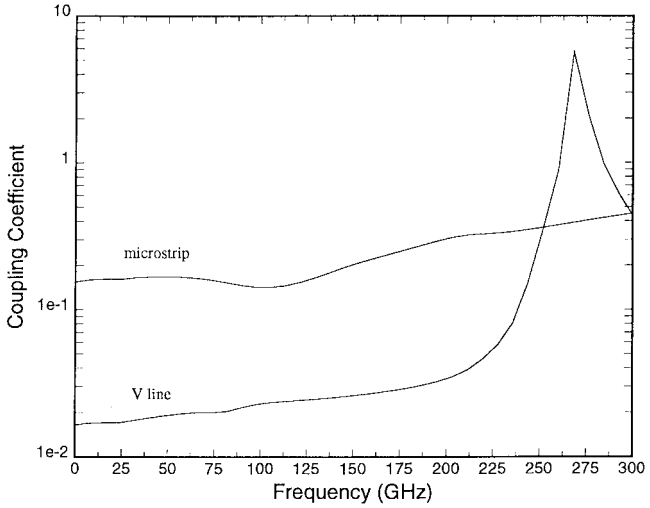

Fig. 13. Coupling coefficient for two identical lines over an extended frequency range. $\alpha = 60°$, W/H = 0.52 and $S = 2$ W.

in phase, while for the odd mode, the current sources are 180° out of phase. From Fig. 10, it is seen that over the lower end of the spectrum, the impedance of the even mode is higher than the single mode, which in turn is higher than the odd mode. This behavior parallels that of the microstrip. However, there is a reversal of this behavior over the upper end of the spectrum. We also notice a smaller deviation in the impedance of the odd and even modes from the single mode in comparison with microstrip line structures. This indicates a lower coupling between the lines. This conclusion is further confirmed by the results of Fig. 11, which shows the coupling coefficient as defined in (4) as a function of frequency for different separation distance S. It is observed that the V line structure gives almost one order of magnitude less coupling than a comparable microstrip structure. Also observed is that the V line provides better coupling performance over an extended frequency range than the microstrip. Notice that above 120 GHz, increasing S has minimal effect on coupling for the microstrip structure whereas in the V line case, the lines continue to have lower coupling as would be the case over the lower end of the spectrum.

Fig. 12 looks at the coupling rate at 80 GHz. As the distance S increases, the V lines decouple at a faster rate than the microstrip. This behavior is similar to that found for microstrip-ridge structures [4] which have a strong topological resemblance to the V line structure.

Finally we look at the behavior of the multiconductor V line structure over an extended frequency range up to 300 GHz. Fig. 13 shows the coupling coefficient for the microstrip

and V line, with $W/H = 0.52$, $\alpha = 60°$ and $S = 2$ W. We notice that the V line structure exhibits a resonance-like behavior at approximately 270 GHz. This implies that relatively high energy is being transferred to the passive line at this frequency. This behavior is understood in the context of coupled cavities. Notice that two adjacent V groves create, in essence, a coupled cavities system. Thus, we expect the V groves to become efficient radiators at wavelengths corresponding to approximately twice the width of the V grove opening. In fact, a series of simulations found that the resonant point is directly related to the width of the V grove, and that the traces play the role of "cavity loads," thus altering the resonance point and the Q. Also it was found that the distance between the two groves affects the Q.

Clearly the application of V lines does not call for the V groves to be efficient radiators, and thus, the V line will have a useful frequency bandwidth beyond which the performance, in multiconductor transmission lines applications, starts to deteriorate. For present applications the performance over the extended frequency range (above 150 GHz) is of little interest since the structure dimensions for any practical applications will always push the resonance behavior beyond the frequency band of interest. However, it suffices to highlight this limitation; one which is not present in the conventional multiconductor microstrip.

IV. Conclusion

In this work, a dynamic analysis of the V transmission line is presented. The Yee-cell based FDTD method was used in conjunction with a recently introduced formulation to accurately model the inclined boundaries present in the structure. The V line main characteristic is the angle of the isosceles triangle, α which can be varied, while having fixed substrate height, to achieve flexibility in the design characteristics. Furthermore, the V line is found to be less dispersive than conventional microstrip lines which allows faster propagation of signals. However, the most pronounced feature of the V line is the low coupling between adjacent lines. This feature makes the V line very attractive for high density packaging.

Acknowledgment

The authors are grateful to the reviewers for the comments that enhanced the quality of this paper.

References

[1] J. Schutt-Aine, "Static analysis of V transmission lines," *IEEE Trans. Microwave Theory Tech.*, vol. 40, pp. 659–663, Apr. 1992.
[2] S. He, A. Z. Elsherbeni, and C. E. Smith, "Decoupling between two conductor microstrip transmission line," *IEEE Trans. Microwave Theory Tech.*, vol. 41, pp. 53–61, Jan. 1993.
[3] N. I. Dib and L. P. B. Katehi, "Impedance calculation for the microshield line," *IEEE Microwave Guide Wave Lett.*, vol. 2, pp. 406–408, Oct. 1992.
[4] A. G. Engel, Jr. and L. Katehi, "Frequency and time domain characterization of microstrip-ridge structures," *IEEE Trans. Microwave Theory Tech.*, vol. 41, pp. 1251–1262, Aug. 1993.
[5] N. Yuan, C. Ruan, and W. Lin, "Analytical analyzes of V, elliptic, and circular-shaped microshield transmission lines," *IEEE Trans. Microwave Theory Tech.*, vol. 42, pp. 855–859, May 1994.
[6] O. M. Ramahi, "Efficient characterization of microstrip structures using higher order boundary operators," in *URSI Radio Sci. Meeting*, Montreal, P.Q., Canada, July 13–18, 1997.
[7] S. Xiao, R. Vahldieck, and H. Jin, "Full-wave analysis of guided wave structures using a novel 2-D FDTD," *IEEE Microwave Guide Wave Lett.*, vol. 2, pp. 165–167, May 1992.
[8] X. Zhang, J. Fang, K. Mei, and Y. Liu, "Calculations of dispersive characteristics of microstrips by the time-domain finite difference method," *IEEE Trans. Microwave Theory Tech.*, vol. MTT-36, pp. 263–267, Feb. 1988.
[9] D. M. Sheen, S. M. Ali, M. D. Abouzahra, and J. A. Kong, "Application of the three-dimensional finite-difference time-domain method to the analysis of planar microstrip circuits," *IEEE Trans. Microwave Theory Tech.*, vol. 38, pp. 849–857, July 1990.
[10] P. Cherry and M. F. Iskander, "FDTD analysis of high frequency electronic interconnection effects," *IEEE Trans. Microwave Theory Tech.*, vol. 43, pp. 2445–2451, Oct. 1995.
[11] P. Mezzanotte, L. Roselli, and R. Sorrentino, "A simple way to model curved metal boundaries in FDTD algorithm avoiding staircase approximation," *IEEE Microwave Guide Wave Lett.*, vol. 5, pp. 267–269, Aug. 1995.
[12] J. Fang and J. Ren, "A locally conformed finite-difference time-domain algorithm of modeling arbitrary shape planar metal strips," *IEEE Trans. Microwave Theory Tech.*, vol. 41, pp. 830–838, May 1993.
[13] I. J. Craddock and C. J. Railton, "A novel finite-difference time-domain algorithm incorporating correction coefficients for curved boundaries," in *Proc. 24th Euro. Microwave Conf.*, Cannes, France, Sept. 1994, pp. 1536–1540.
[14] ——, "Analysis of curved and angled surfaces on a Cartesian mesh using a novel finite-difference time-domain algorithm," *IEEE Trans. Microwave Theory Tech.*, vol. 43, pp. 2460–2465, Oct. 1995.
[15] ——, "Stable inclusion of *a priori* knowledge of field behavior in the FDTD algorithm to the analysis of microstrip lines," in *IEEE Antennas Propagat. Soc. Int. Symp.*, Baltimore, MD, July 1996, vol. 2, pp. 1300–1303.
[16] R. L. Higdon, "Radiation boundary conditions for dispersive waves," *Siam J. Numer. Anal.*, vol. 31, no. 1, pp. 64–100, Feb. 1994.
[17] Z. Bi, K. Wu, C. Wu, and J. Litva, "A dispersive boundary condition for microstrip component analysis using the FD-TD method," *IEEE Trans. Microwave Theory Tech.*, vol. 40, pp. 774–776, Apr. 1992.
[18] V. Betz and R. Mittra, "Comparison and evaluation of boundary conditions for the absorption of guided waves in an FDTD simulation," *IEEE Microwave Guide Wave Lett.*, vol. 2, pp. 499–501, Dec. 1992.
[19] Z. Wu and J. Fang, "Numerical implementation and performance of perfectly matched layer boundary condition for waveguide structures," *IEEE Trans. Microwave Theory Tech.*, vol. 43, pp. 2676–2683, Dec. 1995.
[20] O. M. Ramahi, "Application of the complementary boundary operators in the FDTD solution of planar and printed circuits problems," in *Proc. Progress Electromag. Res. Symp.*, Seattle, WA, July 24–28, 1995.
[21] J. Schutt-Aine, private communications.

Omar M. Ramahi received the B.S. degree in electrical engineering and the B.S. degree in mathematics (with highest honors) from Oregon State University, Corvallis, in 1984, and the M.S. and Ph.D. degrees in electrical engineering from the University of Illinois, Urbana-Champaign, in 1986 and 1990, respectively.

From 1990 to 1993, he was a Post-Doctoral Research Fellow at the University of Illinois, Urbana-Champaign. Since 1993, he has been with Digital Equipment Corporation, Maynard, MA. His interests include computational physics, radiation phenomenon, antennas, microwave and high-speed digital circuits, packaging, and medical applications of electromagnetics. He is the co-author of *EMI/EMC Computational Modeling Handbook*. He has published over 60 conference and journal papers.

Dr. Ramahi is a member of the Engineering Academy.

Atef Z. Elsherbeni (S'84–M'86–SM'91) received the B.Sc. degree in electronics and communications (with honors), the B.Sc. degree in applied physics (with honors), and the M.Eng. degree in electrical engineering, all from Cairo University, Egypt, in 1976, 1979, and 1982, respectively, and the Ph.D. degree in electrical engineering from the University of Manitoba, Winnipeg, Man., Canada, in 1987.

From January to August 1987, he was a Post-Doctoral Fellow with the Electrical Engineering Department, University of Manitoba. He joined the faculty at the University of Mississippi, University, in August 1987, where he is now Professor of Electrical Engineering. From January to August 1996, he was on sabbatical leave at the University of California, Los Angeles (UCLA). His professional interests include microstrip antennas, scattering and diffraction of electromagnetic waves, numerical techniques and computer applications for electromagnetic education.

Dr. Elsherbeni is a member of the Applied Computational Electromagnetic Society, the URSI Commission B, the Electromagnetics Academy, and Sigma Xi. He serves on the editorial boards of the IEEE TRANSACTIONS ON MICROWAVE THEORY AND TECHNIQUES, the *Journal of Electromagnetic Waves and Applications* and *Computer Applications in Electromagnetic Education Journal*.

Charles E. Smith (M'35–LS'86) was born in Clayton, AL, on June 8, 1934. He received the B.E.E., M.S., and Ph.D. degrees from Auburn University, Auburn, AL, in 1959, 1963, and 1968, respectively.

He was a Research Assistant with the Auburn University Research Foundation from 1959 to 1968. In late 1968, he became Assistant Professor of Electrical Engineering, University of Mississippi, University, and Associate Professor in 1969. His main areas of interest are related to the application of electromagnetic theory to microwave circuits and antennas. His recent research has been on the application of numerical techniques to microstrip transmission lines, antenna measurements in lossy media, measurement of electrical properties of materials, CAD in microwave circuits, and data acquisition using network analyzers. He was appointed Chairman of the Department of Electrical Engineering, University of Mississippi, in 1975, and is currently Professor and Chair of this department.